

RESEARCH ARTICLE | DECEMBER 30 2019

Accurate calculation of zero point energy from molecular dynamics simulations of liquids and their mixtures

A. Tiwari; C. Honingh; B. Ensing 



J. Chem. Phys. 151, 244124 (2019)
<https://doi.org/10.1063/1.5131145>



Articles You May Be Interested In

Lattice Boltzmann implementation of the three-dimensional Ben-Naim potential for water-like fluids

J. Chem. Phys. (March 2013)

Influence of reservoir size on the adsorption path in an ideal pore

J. Chem. Phys. (September 2009)

Studying molecular dynamics of the slow, structural, and secondary relaxation processes in series of substituted ibuprofens

J. Chem. Phys. (June 2018)



Order now

 Zurich
Instruments

Freedom to Innovate.

The New VHFLI 200 MHz Lock-in Amplifier.

Orchestrate pulses, triggers, and acquisition as the hub of your experiment.
Discover more – run every signal analysis tool, simultaneously.

Accurate calculation of zero point energy from molecular dynamics simulations of liquids and their mixtures

Cite as: J. Chem. Phys. 151, 244124 (2019); doi: 10.1063/1.5131145

Submitted: 10 October 2019 • Accepted: 18 November 2019 •

Published Online: 30 December 2019



View Online



Export Citation



CrossMark

A. Tiwari,^{1,2,a)} C. Honingh,^{1,2} and B. Ensing^{1,2,b)}

AFFILIATIONS

¹Van't Hoff Institute for Molecular Sciences, Universiteit van Amsterdam, Science Park 904, 1098 XH Amsterdam, The Netherlands

²Amsterdam Center for Multiscale Modeling, Science Park 904, 1098 XH Amsterdam, The Netherlands

^{a)}Electronic mail: a.tiwari@uva.nl

^{b)}Electronic mail: b.ensing@uva.nl

ABSTRACT

The two-phase thermodynamic (2PT) method is used to compute the zero point energy (ZPE) of several liquids and their mixtures. The 2PT method uses the density of states (DoS), which is computed from the velocity autocorrelation (VAC) function obtained from a short classical molecular dynamics trajectory. By partitioning the VAC and the DoS of a fluid into solid and gaslike components, quantum mechanical corrections to thermodynamical properties can be computed. The ZPE is obtained by combining the partition function of the quantum harmonic oscillator with the vibrational part of the solidlike DoS. The resulting ZPE is found to be in excellent agreement with both experimental and *ab initio* results. Solvent effects such as hydrogen bonding and polarization can be included by the utilization of *ab initio* density functional theory based molecular dynamics simulations. It is found that these effects significantly influence the DoS of water molecules. The obtained results demonstrate that the 2PT model is a powerful method for efficient ZPE calculations, in particular, to account for solvent effects and polarization.

Published under license by AIP Publishing. <https://doi.org/10.1063/1.5131145>

I. INTRODUCTION

Quantum chemical calculation of molecular energies has become a standard tool for various research applications, including thermochemistry, catalysis, and reaction kinetics. With constant improvement of commonly used density functional theory (DFT) calculations, the error in molecular energy has reduced to only a few kilocalories per mole requiring other sources of errors to improve as well. One such source of error in many cases has been shown to be quantum nuclear effects, in particular, the zero point energy (ZPE). The ZPE represents the energy of a system at absolute zero, corresponding to the lowest vibrational energy level. Perhaps one of the most important consequences of ZPE is the effect on bond strength as measured by the kinetic isotope effect.^{1–3} The strength of a chemical bond is related to the vibrational energy of that bond. A regular C–H stretch vibration has a frequency of approximately 2900 cm^{-1} ,

corresponding to a ZPE of 17 kJ/mol. When hydrogen is substituted with deuterium, the mass of the atoms doubles, decreasing the C–D stretch vibration to 2100 cm^{-1} , corresponding to a ZPE of approximately 13 kJ/mol. This decrease of 4 kJ/mol means that more energy is required to break a C–D bond compared to the more energetic C–H bond. Chemical reactions on deuterated substrates are thus generally slower than the protonated variant, as the higher energy barrier leads to a lower rate constant.

This effect is even more important in water and aqueous systems. The O–H stretch vibration in water has a frequency of approximately 3700 cm^{-1} , corresponding to a ZPE of 21 kJ/mol, which is quite significant.⁴ D₂O and T₂O have lower stretch frequencies, corresponding to a ZPE of 15 and 12 kJ/mol, respectively. The higher bond strength of D₂O means that it is less likely to self-ionize in comparison to regular H₂O, resulting in a higher pH of 7.43 for D₂O compared to 7.0 for H₂O. Heavy water also forms stronger hydrogen

bonds, as is observed by the increase in the melting point from 273 K for regular water to 277 K for heavy water.⁵

It has also been demonstrated that hydrogen bonding itself affects the zero point energy of solvated molecules.⁴ When a hydrogen bond is formed between two water molecules, the intramolecular vibrations are perturbed, leading to an increased contribution of the bending mode. This consequently leads to an overall decrease in ZPE in the molecule as the vibrational contribution is decreased.⁶ Hydrogen bonding organic molecules are also affected by this ZPE contribution. It has been shown that ring substitutions in anisole change the structure of the hydrogen bond, this in turn affects the zero point energy of the molecule as the H-bond structures perturb the bond vibrations to a varying degree.⁷ All of these effects suggest the need for a thorough study of various liquid systems and analyze the effect of solvation on the ZPE of dissolved molecules by comparison with the gas phase results obtained from DFT calculations.

It is possible to incorporate nuclear quantum effects through path integral based methods such as centroid molecular dynamics,⁸ ring polymer molecular dynamics,⁹ and Feynman-Kleinert quasi-classical Wigner¹⁰ methods, but these require expensive calculations that are not practical for larger molecular systems.

To obtain quantum corrected results without the need of enormous amounts of computational time, a method was proposed based on the density of states (DoS) of a system.¹¹ The DoS can be obtained through a Fourier transform of the mass-weighed velocity autocorrelation (VAC) function computed from a molecular dynamics trajectory. The DoS represents the density of vibrational normal modes of a system, which means that for harmonic systems, it is directly related to thermodynamic properties through quantum statistics. The main limitation of this method is that it assumes that the molecular system is fully harmonic and has no density at zero frequency. While this is true for solids, liquids have a finite DoS at frequency zero, which corresponds to the diffusive behavior of the liquid and would result in infinite entropy and energy at this frequency.

Based on the previous work of Berens *et al.*,¹¹ an improved method was proposed by Lin *et al.*, known as the 2PT method,¹² which decomposes the liquid DoS into solid and gaseous (diffusive) components. This was based on the observation that the liquid DoS can be seen as a superposition of the solid and diffusive DoS. Decomposing the liquid density of states thus allows for separate computation of the low frequency anharmonic (classical) and high frequency harmonic (quantum) effects such as ZPE.

The 2PT method has been extensively used to calculate various thermodynamic properties such as the entropy of solids, liquids, and their mixtures.^{13–22} In addition, it was proposed that various thermodynamic properties can be converged in 20 ps of classical MD simulations. Here, we propose to use the 2PT method to obtain the ZPE and perform extensive benchmark calculations for several liquids and their mixtures. We also test the convergence time and the chemical accuracy for ZPE calculations as explained hereafter.

II. THEORETICAL BACKGROUND

A. Density of states

The DoS of a system can be obtained from the mass-weighed velocity autocorrelation function (VAC),

$$C(t) = \sum_{j=1}^N \sum_{k=1}^3 m_j \langle v_j^k(t') v_j^k(t'+t) \rangle_t, \quad (1)$$

in which m_j is the mass of atom j , $v_j^k(t')$ is the velocity of atom j along axis k at initial time t' , and $v_j^k(t'+t)$ is the velocity of the same atom after a time delay t . The brackets indicate the ensemble average over initial times t' . N is the number of particles in the system. A typical velocity autocorrelation function is shown in Fig. 1, which has been normalized by dividing by $\langle v(0)^2 \rangle$ so that the function is one when the delayed velocity is equal to the initial velocity, such as at zero time lag. At larger time lags, the function quickly decays to zero as the function loses its memory due to the random collisions that underlie the particle's diffusive motion. Because the VAC represents the periodicity of a system in the time domain, a Fourier transform can be used to obtain these periodic normal modes in the frequency domain; the density of states, $S(\nu)$, as follows:

$$S(\nu) = \frac{2}{k_B T} \lim_{\tau \rightarrow \infty} \int_{-\tau}^{+\tau} C(t) \exp(-i2\pi\nu t) dt, \quad (2)$$

where T is the temperature of the system and k_B is Boltzmann's constant. The physical meaning of the density of states at a specific frequency ν is that it represents the density of normal modes at that frequency. Specific domains of the DoS can thus be related to the chemical and physical properties of the molecule in question. The high frequency range is dominated by vibrational motion; the DoS in this region can thus be compared to the infrared absorption spectrum of a molecule. Lower frequencies correspond to other types of motions such as rotation and translation. A typical density of states function is shown in Fig. 2. The characteristic IR vibrations can clearly be seen, such as the C-H stretch at 3000 cm^{-1} . Rotational and translational normal modes are contained in the bump below 100 cm^{-1} , which does not occur in a normal IR spectrum. Because the DoS is a measure of the density of normal modes, integration over the entire function gives the total amount of normal modes of the system; the degrees of freedom

$$\int_0^\infty S(\nu) d\nu = 3N. \quad (3)$$

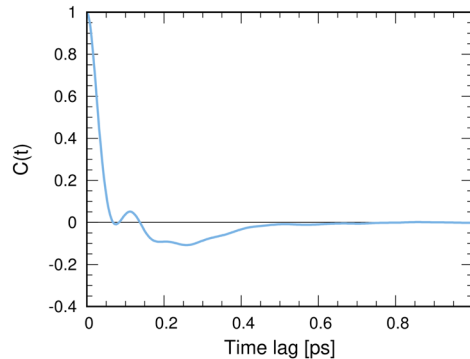


FIG. 1. Velocity autocorrelation function of TIP3P water, normalized to one at zero time lag.

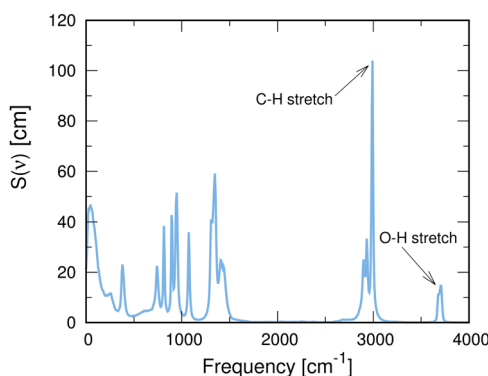


FIG. 2. The density of states of liquid ethanol.

The density of states at the origin, $S(v = 0)$, corresponds to the diffusive modes of the system. It can be used to calculate the self-diffusion coefficient of a liquid as follows:

$$D = \frac{S(0)k_B T}{12Nm}, \quad (4)$$

wherein N is the number of particles with mass m . With the obtained density of states function and the assumption that the system is fully harmonic, the partition function of a system can be obtained using various models, such as the Debye theory of crystals or the quantum harmonic oscillator.^{11,23} However, the application of such simple models is not straightforward to fluids since they exhibit anharmonicity and diffusion.

B. The 2PT method

The main limitation of the quantum harmonic oscillator approximation, discussed hereafter in Sec. II C, is the assumption that the system is completely harmonic. This is not a problem for highly crystalline solids but presents issues when applied to amorphous liquids and gasses. One of these issues is the nonzero density of states at $v = 0$ due to diffusion and anharmonicity. To account for the anharmonic motions in liquids, a refined method was proposed by Lin *et al.*, which splits the density of states into the solid and gaseous components.¹² This was based on the observation that the liquid DoS resembles a superposition of the solid and gaseous states. By decomposing the DoS, it is possible to obtain a fully harmonic component (the solid DoS) and an anharmonic component (the gaseous DoS), onto which the appropriate weighing functions can be used to further calculate thermodynamic properties

$$S_{\text{liquid}}(v) = S_{\text{gas}}(v) + S_{\text{solid}}(v). \quad (5)$$

In order to decompose the DoS, however, one of the components has to be computed analytically. This is accomplished by modeling the gaslike component as a hard sphere fluid. The velocity autocorrelation function of a hard sphere gas can be calculated analytically as follows:

$$C_{HS}(t) = \frac{3k_B T}{m} \exp(-\alpha t), \quad (6)$$

in which α is the Enskog friction constant pertaining in the hard sphere model. By applying the Fourier transforms as described in

Sec. II A, an analytic form of the hard sphere DoS and, therefore, the gaslike DoS can be obtained as follows:

$$S_{HS}(v) = S_{\text{gas}}(v) = \frac{S_0}{1 + \left[\frac{S_0 \pi v}{6fN} \right]^2}, \quad (7)$$

where S_0 is the total density of states at $v = 0$. Here, f is the fluidity of the system, i.e., the fraction of particles N corresponding to the diffusive hard sphere fluid. The fluidity is proportional to the diffusivity Δ of a system, which can be calculated from the self-diffusion,

$$\Delta(T, \rho, m, S_0) = \frac{2S_0}{9N} \left(\frac{\pi k_B T}{m} \right)^{1/2} \rho^{1/3} \left(\frac{6}{\pi} \right)^{2/3}. \quad (8)$$

An expression for the fluidity f can then be obtained by relating the diffusivity of the system to the pure hard sphere diffusivity with the Carnahan-Starling equation of state,

$$2 \left(\frac{f^5}{\Delta^3} \right)^{3/2} - 6 \left(\frac{f^5}{\Delta^3} \right) - \left(\frac{f^7}{\Delta^3} \right)^{1/2} + 6 \left(\frac{f^5}{\Delta^3} \right)^{1/2} + 2f = 2. \quad (9)$$

Because the 2PT method depends on the motion of atoms, molecules with more than one atom require decomposition into the primary degrees of motion. This is accomplished by decomposing the velocity into translational, rotational, and vibrational components as follows:

$$v(t) = v_{\text{trans}}(t) + v_{\text{rot}}(t) + v_{\text{vib}}(t). \quad (10)$$

The translational component of the velocity is obtained by calculating the mass weighed velocity for each molecule,

$$v_{\text{trans}}(t) = \frac{1}{M_i} \sum_j m_j v_j(t), \quad (11)$$

where m_j is the mass of atom j and M_i is the total mass of all atoms j in molecule i . The rotational component can be computed from the angular velocity ω of each molecule i ,

$$v_{\text{rot}}(t) = \omega(t) \times v(t). \quad (12)$$

The angular velocity is obtained from the inverse moment of inertia tensor I_i^{-1} and the angular momentum $L(t)$ of each molecule,

$$\begin{aligned} \omega(t) &= I_i^{-1} \times L(t), \\ L(t) &= \sum_j m_j (r_j \times v_j(t)), \end{aligned} \quad (13)$$

where r_j is the distance of an atom to the center of mass of the molecule. The vibrational velocity is then obtained by subtracting the rotational and translational components from the total velocity,

$$v_{\text{vib}}(t) = v(t) - v_{\text{trans}}(t) - v_{\text{rot}}(t). \quad (14)$$

The resulting density of states after decomposition into a solid and diffusive component is shown in Fig. 3(a); diffusive effects are only relevant at extremely low frequencies, whereas the remaining major

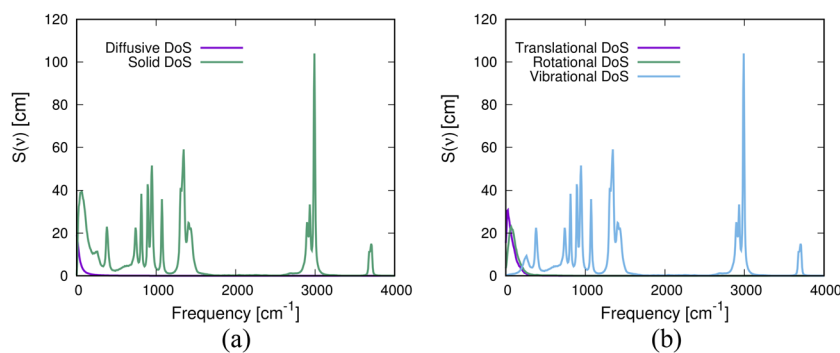


FIG. 3. The decomposed density of states of liquid ethanol: (a) the solid and diffusive states and (b) the different velocity components.

part of the DoS is considered as solid (and therefore harmonic). Figure 3(b) depicts the density of states of the various molecular motions. Rotation and translation dominate the lower frequencies, while anything above 500 cm^{-1} is the result of vibrations.

C. Zero point vibrational energy

The zero-point energy results from the uncertainty principle. If the lowest possible energy state would have zero energy, both its potential and kinetic energies would have to be zero. Zero kinetic energy would mean that the momentum would be exactly zero; therefore, the uncertainty in the momentum (Δp) as well as in the position (Δx) would be zero, which is not allowed according to the Heisenberg uncertainty principle²⁴ as depicted by Eq. (15). Hence, the need for a nonzero ground-state energy,

$$\Delta_x \Delta_p \geq \frac{1}{2}\hbar. \quad (15)$$

In the 2PT method, molecular vibrations are represented as quantum harmonic oscillators, which means that the zero point energy of molecules can be calculated from the lowest energy level of the corresponding harmonic oscillator. The permitted energy levels can be calculated from the Schrödinger equation of a quantum harmonic oscillator,

$$E_n = \left(n + \frac{1}{2}\right)\hbar\omega = \left(n + \frac{1}{2}\right)hv, \\ \omega = \left(\frac{k_f}{m}\right)^{1/2}, \quad v = \frac{\omega}{2\pi}, \quad (16)$$

where ω is the oscillation frequency defined in terms of the force constant k_f and mass m . When a system is considered with only classical mechanics, the energy E of a linear harmonic oscillator can have any value. However, a more precise quantum mechanical description would lead to a nonzero ground state energy, at energy level $n = 0$, which is

$$E_0 = \frac{1}{2}hv. \quad (17)$$

For a group of atoms that constitutes a set of normal modes, the zero-point energy of each mode can be determined independently; thus, the total zero point energy can be obtained using

$$E^{ZP} = \sum_{i=1}^{3N-6} \frac{1}{2}hv_i. \quad (18)$$

The density of states represents the mass-weighed distribution of normal modes of a molecular system; the vibrational component, $S_{vib}(v)$, of the DoS can thus be used to calculate the ZPE of a system,

$$E^{ZP} = \int_0^{\infty} S_{vib}(v) \frac{hv}{2} dv. \quad (19)$$

Because the ZPE represents vibrations at absolute zero, it is problematic to obtain experimental values. Instead, the reported experimental values are extrapolated results from spectroscopic constants.²⁵ This makes accurate and fast theoretical predictions desirable, which serves the motivation of this article.

III. COMPUTATIONAL METHOD

A. Forcefield MD simulations

Molecular dynamics simulations were carried out with the open source LAMMPS software package.²⁶ Initial configurations of 1000 solvent molecules were generated using the packmol software package.²⁷ The atomic interactions were modeled with the General Amber Force Field (GAFF).²⁸ The electrostatic interactions were cutoff at a distance of 10 \AA and augmented with the particle-particle-particle-mesh long-range solver.²⁹ The partial charges of the solvent molecules were fitted using the restrained electrostatic potential (RESP) model, which uses Hartree Fock (HF) calculations to obtain accurate charge distributions for molecules.³⁰ RESP charges were calculated with the Gaussian software package³¹ at the HF/6-31G* level of theory. The initial box configurations were warmed up to a temperature of 300 K in the NVT ensemble using a Nosé–Hoover thermostat over the course of 0.1 ns with a 1 fs time step for the outer time step. A four layer RESPA multi-time step algorithm was used to evaluate middle range interactions ($5.25\text{--}9.0\text{ \AA}$) twice per time step, short range interactions ($0\text{--}5.25\text{ \AA}$) four times per time step, and intramolecular interactions eight times per time step. The systems were then further equilibrated in both the NPT ensemble at 1 bar and NVT at 300 K for 1 ns each.

B. DFT-MD simulations

ZPE calculations were also tested using density functional theory based molecular dynamics (DFT-MD) simulations, where the electronic structure and hence the energy and forces are computed

at every time step using DFT, instead of a force field potential. Despite a large increase in computational power required, DFT-MD offers several advantages compared to forcefield simulations. Chemical processes involving bond breaking or forming, such as proton transfer, are not possible in standard forcefield simulations, thus preventing accurate analysis of hydronium ions and other reactive species. Polarization effects are also not included in the forcefield simulations, limiting the effects of solvents and hydrogen-bonding on molecular vibrations. The open source software package CP2K was used to perform DFT-MD simulations.³² Due to the increased cost of the simulation, a box with 128 molecules was used. The exchange correlation (XC) was computed with the BLYP^{33,34} functional using the TZV2P³⁵ basis set, with DFT-D3 dispersion correction.³⁶ The norm-conserving pseudopotentials of Goedecker *et al.* (GTH)³⁷ were applied to replace the core electrons. The simulations were performed in the NVT ensemble at a temperature of 330 K with a 0.5 fs time step. A higher temperature 330 K was used to counter the slow dynamics of BLYP at 300 K.³⁸

As discussed in the theoretical background, the 2PT method obtains results from the density of states, which is in turn calculated from the velocity autocorrelation function. To obtain accurate results for the density of states, velocities should be sampled to at least double the frequency of the fastest molecular vibration. For liquids, a limit can be set at 4000 cm⁻¹ as this accounts for nearly all IR absorption bands. This frequency corresponds to a period of approximately 8 fs; thus positions and velocity's must be sampled at least every 4 fs.

IV. RESULTS

A. Bulk solvents

A total of six solvents were analyzed on their performance in reproducing accurate results for the zero point energy with the 2PT method. These results were then compared to the experimental values, obtained from the NIST Standard Reference Database.³⁹ As described in the theoretical background, the zero point energy cannot be measured directly experimentally. The extrapolations used in the NIST database are of very high quality, however, and can thus be viewed as accurate.

As demonstrated in Table I, the 2PT method can produce the zero point energy of pure liquids with very high accuracy, deviating from the experimental values by only 2 kJ/mol at most, the

TABLE I. Zero point energies (in kJ/mol) computed with the 2PT method for six liquids using the GAFF forcefield and for DFT/BLYP+D3 water (bottom row). Our MD results are compared to gas-phase DFT calculations and experimental numbers.³⁹

Molecule	2PT	Gas phase	Experiment
Ethyl acetate	310.40	298.35	308.67
DMF	258.75	259.10	259.83
Ethanol	202.15	210.40	202.98
Acetonitrile	114.29	114.60	115.11
Chloroform	51.96	50.03	51.36
Water (TIP3P)	48.86	54.43	53.88
Water (BLYP)	49.96	54.43	53.88

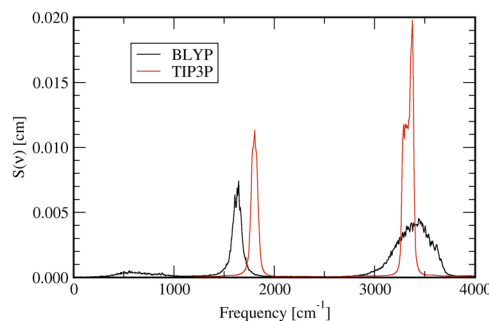


FIG. 4. The vibrational density of states of liquid water, showing the much broader distributions of the DFT BLYP-D3 model compared to the TIP3P forcefield model.

exception being water, which performs significantly worse than the other solvents. To assess the effect of bulk solvent on the ZPE, DFT gas phase calculations of a single molecule were also performed with the Gaussian 09 software package⁴⁰ at the BLYP/6-311G* level of theory. Zero point energy values obtained with the Gaussian package perform slightly worse compared to the experimental values. This in part can be attributed to the inclusion of the solvent effects in the forcefield simulations that are used in the 2PT method.

Including polarization and higher order many body effects using DFT-MD does not influence much the value of the ZPE, as calculated by the 2PT method, as shown in Table I. The similarity between the TIP3P and BLYP results might initially indicate that polarization effects do not significantly influence the zero point energy. However, closer examination of the DoS of the classical TIP3P water and BLYP water in Fig. 4 shows that BLYP water exhibits significant peak broadening, whereas TIP3P has sharp and defined peaks. This difference in DoS is caused by the way that Coulombic interactions are calculated in both models. Classical TIP3P water uses a constant point charge for each atom, whereas DFT-MD computes the electron density at each simulation step. Polarization effects significantly influence molecular properties such as bond strength, hydrogen bonding strengths, and the vibrational frequency.⁴¹ This allows BLYP water to occupy a much broader range of vibrational frequencies compared to the forcefield models. The remarkable resemblance of the ZPE between the TIP3P water and the BLYP-D3 water seems therefore somewhat fortuitous.

TABLE II. Zero point energies (in kJ/mol) computed with the 2PT method for five ethanol-water mixtures, where *x* is the mole fraction of ethanol. Our MD results are compared to the ideally mixed experimental numbers, as explained in the text.

<i>x</i>	2PT	Experiment	Difference
0.96	193.32	196.09	2.77
0.75	159.66	164.25	4.59
0.50	120.68	126.36	5.68
0.25	83.42	88.46	5.01
0.10	60.32	65.72	5.40

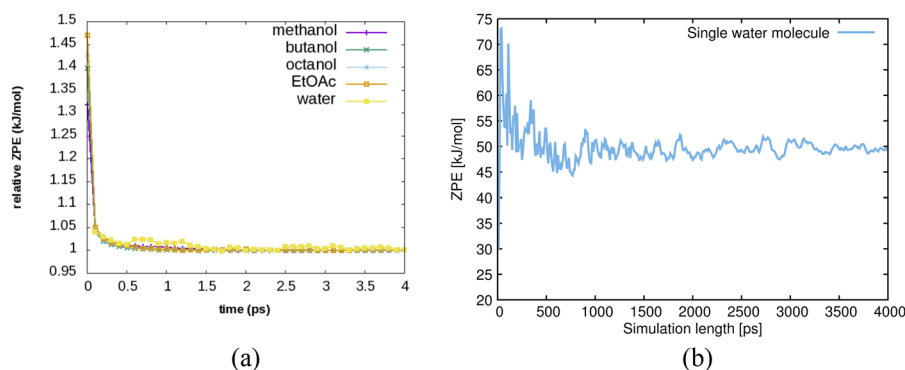


FIG. 5. Convergence of the ZPE computed with the 2PT methods for systems of different sizes: (a) systems containing 1000 molecules and (b) a single water molecule (in a system of 1000 molecules).

B. Mixtures of solvents

Earlier studies utilizing the 2PT method have concluded that the method can effectively capture the excess Gibbs free energy in mixtures of classical solvents.⁴² It is, therefore, worth investigating whether similar observations can be made for the ZPE of solvent mixtures. To this end, ethanol-water mixtures with varying concentrations were run with the same conditions as the bulk solvents (1000 molecules, GAFF force field, 300 K, NVT ensemble). The obtained zero point energy values were then compared to the ideal mixing [using Eq. (20)] of the experimental numbers for the pure liquids, where the ZPE of the each molecular species is weighed by the molar fraction,

$$E^{\text{ZP}} = \sum_i x_i E_i^{\text{ZP}}. \quad (20)$$

The results presented in Table II demonstrate that mixing water and ethanol decreases the overall zero point energy of the system. IR spectroscopy studies on ethanol water mixtures have demonstrated that hydrogen bonding between the two molecules results in an overall decrease in intensity of the O–H stretch vibration.⁴³ This is a result of electronic interactions between the molecules that are not captured accurately as the polarization effects are ignored in the forcefield simulations performed. Ethanol water mixtures are also generally known to reduce in volume due to the nonideal behavior of mixtures; these effects have previously been captured by the 2PT method and shown to influence the entropy and free energy.⁴²

C. Performance and efficiency of the 2PT method

The advantage of the 2PT method is the efficiency with which computing various thermodynamic properties, such as free energy,

entropy, and heat capacity, is possible.^{44–46} Trajectories of only 20 ps are required to obtain the full convergence of these properties, although no benchmarks of ZPE convergence with the 2PT approach have been published to the best of our knowledge.

Figure 5 shows that for large molecular systems, the ZPE converges very quickly; after a simulation time of only 1 ps, a stable value is obtained. This quick convergence is in part caused by the size of the system; the average of 1000 molecules is calculated. Convergence for individual molecules requires longer simulation lengths, as shown in Fig. 5(b); after 1000 ps, a stable result is obtained.

The primary reason to decompose the liquid DoS in a solid and diffusive component is to deal with the anharmonicities in the liquid. This decomposition is based on a hard-sphere approximation of the liquid, which depends on the fluidity of the system following Eqs. (8) and (9). To analyze the performance of the decomposition, the ZPE and the DoS were calculated for ethanol boxes at different temperatures, where it is expected that the gaslike fraction increases at higher temperatures. Because the ZPE represents the energy of a molecule in its lowest energy state, it should be independent of temperature.

Table III demonstrates that the 2PT method can accurately compute the ZPE across a wide range of temperatures, deviating by only a few kilocalories per mole even at extreme temperatures. The increased gaslike nature at high temperature is accounted for by the fluidity factor, which describes the fraction of the system corresponding to diffusive behavior. Figures 6(a) and 6(b) show the “solid ethanol” contributions that have near negligible diffusive components. Figures 6(c) and 6(d) show significant diffusive contributions below a frequency of 25 cm⁻¹, arising from the more anharmonic and fluidic nature of the system.

TABLE III. ZPE and fluidity of ethanol at various temperatures.

Temperature (K)	ZPE (kJ/mol)	Fluidity factor	Diffusion coefficient (10 ⁻⁵ cm ² /s)
50	201.15	0.033	0.013
100	202.73	0.046	0.036
300	202.15	0.25	2.32
500	202.89	0.63	20.15
1000	200.26	0.86	105.90

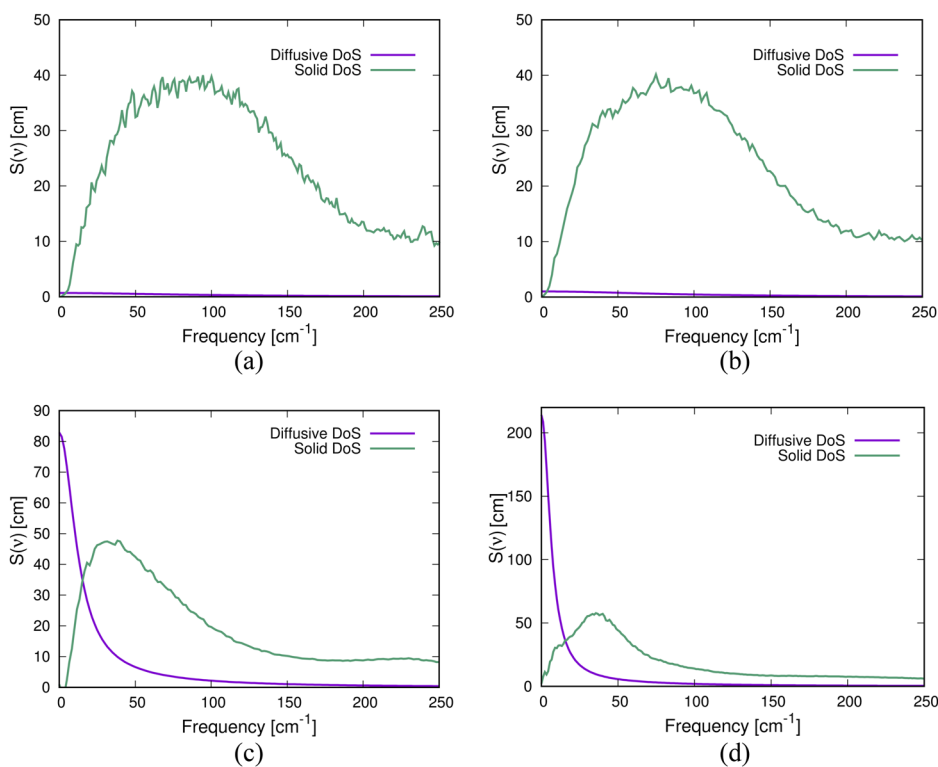


FIG. 6. DoS decomposition in the solid and gaslike (i.e., diffusive) contributions: (a) $T = 50\text{ K}$, (b) $T = 100\text{ K}$, (c) $T = 500\text{ K}$, and (d) $T = 1000\text{ K}$.

V. CONCLUSIONS

We have used the 2PT method to accurately calculate the zero point energy of several pure liquids and mixtures from short MD trajectories. Simulations of bulk solvents require only a picosecond of simulation time as the ZPE can be averaged over all the molecules in the box. However, calculating the ZPE for individual molecules requires a much longer simulation time of 1000 ps to fully converge. For most pure liquids investigated here, the ZPE is not affected very strongly by solvent effects, as seen from the already good performance of the ZPE calculation of the isolated (gas phase) molecule compared to the experimental number. The exceptions are ethanol and ethyl acetate, for which the gas phase estimates are 7.4 kJ/mol (too high) and 10.3 kJ/mol (too low), respectively, whereas the PT2 full solvent result is within 2 kJ/mol. Remarkably, for liquid water, the opposite is observed: the gas phase number is in good agreement with the experiment, whereas the 2PT method applied to liquid TIP3P water results in an almost 10% too low number. Moreover, the 2PT estimate from DFT BLYP-D3 water agrees with the TIP3P result. Considering the excellent performance of the PT2 approach for the other liquids, it may be worthwhile to reexamine the experimental estimate for liquid water. For various mixtures of ethanol and water, the ZPE estimate is seen to be somewhat too low, which can be partly attributed to the too low ZPE of water and partly to the neglect of nonideal mixing in the calculation of the experimental number. The 2PT approach to ZPE calculations can be particularly powerful to estimate these nuclear quantum effects onto the thermodynamics of complex liquids or chemical reactions, such as acid/base reactions. Although within the context of the DFT-MD

simulation, the calculation of the ZPE of a single acid or conjugate base molecule in water solvent might still require prohibitively long trajectories.

ACKNOWLEDGMENTS

This work was carried out on the Dutch national e-infrastructure with the support of SURF Cooperative and is part of the Industrial Partnership Programme (IPP) “Computational sciences for energy research” of the NWO-I, which is part of the Netherlands Organisation for Scientific Research (NWO). This research programme is co-financed by Shell Global Solutions International B.V.

REFERENCES

1. J. Bigeleisen and M. Wolfsberg, in *Advances in Chemical Physics*, edited by I. Prigogine and P. Debye (John Wiley & Sons. Inc., New York, 2007), Vol. 1, pp. 15–76.
2. F. Westheimer, *Chem. Rev.* **61**, 265 (1961).
3. Y. P. Liu, D. H. Lu, A. Gonzalez-Lafont, D. G. Truhlar, and B. C. Garrett, *J. Am. Chem. Soc.* **115**, 7806 (1993).
4. M. Ceriotti, W. Fang, P. G. Kusalik, R. H. McKenzie, A. Michaelides, M. A. Morales, and T. E. Markland, *Chem. Rev.* **116**, 7529 (2016).
5. C. McBride, J. L. Aragones, E. G. Noya, and C. Vega, *Phys. Chem. Chem. Phys.* **14**, 15199 (2012).
6. J. K. Gregory and D. C. Clary, *J. Phys. Chem.* **100**, 18014 (1996).
7. H. C. Gottschalk, J. Altnöder, M. Heger, and M. A. Suhm, *Angew. Chem., Int. Ed.* **55**, 1921 (2016).
8. J. Cao and G. A. Voth, *J. Chem. Phys.* **100**, 5106 (1994).

- ⁹I. R. Craig and D. E. Manolopoulos, *J. Chem. Phys.* **121**, 3368 (2004).
- ¹⁰K. K. Smith, J. A. Poulsen, G. Nyman, and P. J. Rossky, *J. Chem. Phys.* **142**, 244112 (2015).
- ¹¹P. H. Berens, D. H. Mackay, G. M. White, and K. R. Wilson, *J. Chem. Phys.* **79**, 2375 (1983).
- ¹²S.-T. Lin, M. Blanco, and W. A. Goddard III, *J. Chem. Phys.* **119**, 11792 (2003).
- ¹³A. Debnath, B. Mukherjee, K. Ayappa, P. K. Maiti, and S.-T. Lin, *J. Chem. Phys.* **133**, 174704 (2010).
- ¹⁴C. Zhang, L. Spanu, and G. Galli, *J. Phys. Chem. B* **115**, 14190 (2011).
- ¹⁵A. Teweldeberhan and S. Bonev, *Phys. Rev. B* **83**, 134120 (2011).
- ¹⁶S.-N. Huang, T. A. Pascal, W. A. Goddard III, P. K. Maiti, and S.-T. Lin, *J. Chem. Theory Comput.* **7**, 1893 (2011).
- ¹⁷T. A. Pascal, W. A. Goddard III, P. K. Maiti, and N. Vaidehi, *J. Phys. Chem. B* **116**, 12159 (2012).
- ¹⁸T. A. Pascal and W. A. Goddard III, *J. Phys. Chem. B* **116**, 13905 (2012).
- ¹⁹T. A. Pascal, D. Schärf, Y. Jung, and T. D. Kühne, *J. Chem. Phys.* **137**, 244507 (2012).
- ²⁰J. Wang, B. Chakraborty, and J. Eapen, *Phys. Chem. Chem. Phys.* **16**, 3062 (2014).
- ²¹M. A. Caro, T. Laurila, and O. Lopez-Acevedo, *J. Chem. Phys.* **145**, 244504 (2016).
- ²²T. A. Pascal, K. H. Wujcik, D. R. Wang, N. P. Balsara, and D. Prendergast, *Phys. Chem. Chem. Phys.* **19**, 1441 (2017).
- ²³D. McQuarrie, *Statistical Mechanics* (Harper & Row 1976).
- ²⁴W. Heisenberg, *Original Scientific Papers Wissenschaftliche Originalarbeiten* (Springer, 1985), pp. 478–504.
- ²⁵K. K. Irikura, R. D. Johnson III, R. N. Kacker, and R. Kessel, *J. Chem. Phys.* **130**, 114102 (2009).
- ²⁶S. Plimpton, *J. Comput. Phys.* **117**, 1 (1995).
- ²⁷L. Martínez, R. Andrade, E. G. Birgin, and J. M. Martínez, *J. Comput. Chem.* **30**, 2157 (2009).
- ²⁸J. Wang, R. M. Wolf, J. W. Caldwell, P. A. Kollman, and D. A. Case, *J. Comput. Chem.* **25**, 1157 (2004).
- ²⁹R. W. Hockney and J. W. Eastwood, *Computer Simulation Using Particles* (CRC Press, 1988).
- ³⁰J. Wang, P. Cieplak, and P. A. Kollman, *J. Comput. Chem.* **21**, 1049 (2000).
- ³¹M. Frisch, G. Trucks, H. Schlegel, G. Scuseria, M. Robb, J. Cheeseman, G. Scalmani, V. Barone, G. Petersson, H. Nakatsuji *et al.*, *GAUSSIAN 09*, Revision E.01, Gaussian, Inc., Wallingford, CT, 2016.
- ³²S. Andermatt, J. Cha, F. Schiffmann, and J. VandeVondele, *J. Chem. Theory Comput.* **12**, 3214 (2016).
- ³³A. D. Becke, *Phys. Rev. A* **38**, 3098 (1988).
- ³⁴C. Lee, W. Yang, and R. G. Parr, *Phys. Rev. B* **37**, 785 (1988).
- ³⁵J. VandeVondele and J. Hutter, *J. Chem. Phys.* **127**, 114105 (2007).
- ³⁶S. Grimme, J. Antony, S. Ehrlich, and H. Krieg, *J. Chem. Phys.* **132**, 154104 (2010).
- ³⁷S. Goedecker, M. Teter, and J. Hutter, *Phys. Rev. B* **54**, 1703 (1996).
- ³⁸M. J. Gillan, D. Alfè, and A. Michaelides, *J. Chem. Phys.* **144**, 130901 (2016).
- ³⁹R. D. Johnson III, “NIST Computational Chemistry Comparison and Benchmark Database, Release 20,” NIST Standard Reference Database Number 101, August 2019, <http://cccbdb.nist.gov/>.
- ⁴⁰M. J. Frisch, G. W. Trucks, H. B. Schlegel, G. E. Scuseria, M. A. Robb, J. R. Cheeseman, G. Scalmani, V. Barone, G. A. Petersson, H. Nakatsuji, X. Li, M. Caricato, A. V. Marenich, J. Bloino, B. G. Janesko, R. Gomperts, B. Mennucci, H. P. Hratchian, J. V. Ortiz, A. F. Izmaylov, J. L. Sonnenberg, D. Williams-Young, F. Ding, F. Lipparini, F. Egidi, J. Goings, B. Peng, A. Petrone, T. Henderson, D. Ranasinghe, V. G. Zakrzewski, J. Gao, N. Rega, G. Zheng, W. Liang, M. Hada, M. Ehara, K. Toyota, R. Fukuda, J. Hasegawa, M. Ishida, T. Nakajima, Y. Honda, O. Kitao, H. Nakai, T. Vreven, K. Throssell, J. A. Montgomery, Jr., J. E. Peralta, F. Ogliaro, M. J. Bearpark, J. J. Heyd, E. N. Brothers, K. N. Kudin, V. N. Staroverov, T. A. Keith, R. Kobayashi, J. Normand, K. Raghavachari, A. P. Rendell, J. C. Burant, S. S. Iyengar, J. Tomasi, M. Cossi, J. M. Millam, M. Klene, C. Adamo, R. Cammi, J. W. Ochterski, R. L. Martin, K. Morokuma, O. Farkas, J. B. Foresman, and D. J. Fox, *GAUSSIAN 09*, Revision B.01, Gaussian, Inc., Wallingford, CT, 2009.
- ⁴¹F. J. Luque, F. Dehez, C. Chipot, and M. Orozco, *Wiley Interdiscip. Rev.: Comput. Mol. Sci.* **1**, 844 (2011).
- ⁴²P.-K. Lai, C.-M. Hsieh, and S.-T. Lin, *Phys. Chem. Chem. Phys.* **14**, 15206 (2012).
- ⁴³S. Burikov, T. Dolenko, S. Patsaeva, Y. Starokurov, and V. Yuzhakov, *Mol. Phys.* **108**, 2427 (2010).
- ⁴⁴S.-T. Lin, P. K. Maiti, and W. A. Goddard III, *J. Phys. Chem. B* **114**, 8191 (2010).
- ⁴⁵T. A. Pascal, S.-T. Lin, and W. A. Goddard III, *Phys. Chem. Chem. Phys.* **13**, 169 (2011).
- ⁴⁶L. Yang and S.-T. Lin, *AIChE J.* **61**, 2298 (2015).